

Molecular dynamics simulation of the dielectric constant of water: The effect of bond flexibility

Gabriele Raabe¹ and Richard J. Sadus^{2,a)}

¹*Institut für Thermodynamik, Technische Universität Braunschweig, Hans-Sommer-Str. 5, 38106 Braunschweig, Germany*

²*Centre for Molecular Simulation, Swinburne University of Technology, PO Box 218, Hawthorn, Victoria 3122, Australia*

(Received 31 March 2011; accepted 24 May 2011; published online 15 June 2011)

The role of bond flexibility on the dielectric constant of water is investigated via molecular dynamics simulations using a flexible intermolecular potential SPC/Fw [Y. Wu, H. L. Tepper, and G. A. Voth, *J. Chem. Phys.* **128**, 024503 (2006)]. Dielectric constants and densities are reported for the liquid phase at temperatures of 298.15 K and 473.15 K and the supercritical phase at 673.15 K for pressures between 0.1 MPa and 200 MPa. Comparison with both experimental data and other rigid bond intermolecular potentials indicates that introducing bond flexibility significantly improves the prediction of both dielectric constants and pressure–temperature–density behavior. In some cases, the predicted densities and dielectric constants almost exactly coincide with experimental data. The results are analyzed in terms of dipole moments, quadrupole moments, and equilibrium bond angles and lengths. It appears that bond flexibility allows the molecular dipole and quadrupole moment to change with the thermodynamic state point, and thereby mimic the change of the intermolecular interactions in response to the local environment. © 2011 American Institute of Physics. [doi:10.1063/1.3600337]

I. INTRODUCTION

The properties of water have a key role in many biological, chemical, physical, and technical processes. The diverse, and sometime anomalous, thermophysical properties of water are well established experimentally.¹ In principle, any thermodynamic property can be predicted via molecular simulation² using a suitable intermolecular potential and many such potentials for water have been proposed.³

Arguably, the dielectric constant (ϵ_r) or relative permittivity represents a very good test for the accuracy of an intermolecular potential because it is a property that incorporates both short and long-range spatial and orientational correlations. The dielectric constant is a state point dependent property of a substance, which mitigates the strength of Coulombic interactions that would otherwise be experienced in a vacuum ($\epsilon_r = 1$). In contrast to both non-polar systems and other molecules with a similar, or indeed larger, dipole moment, water is known to have a high dielectric constant (e.g., $\epsilon_r = 78.5$ at 298 K).⁴ This partly explains the efficacy of water as a solvent; Coulombic interactions between ions dissolved in water are greatly reduced preventing conglomeration into a crystal.

The most common intermolecular potentials for water involve rigid bonds with intermolecular interaction obtained from a combination of Lennard-Jones interaction between the oxygen atoms and Coulombic interaction between various partial charges distributed either on or near the oxygen and hydrogen atoms. At ambient conditions, the simple point charge SPC (Ref. 5) ($\epsilon_r = 63$ at 300 K) (Ref. 6) and extended SPC/E

(Ref. 7) ($\epsilon_r = 70.7$ (Ref. 8) or alternatively 63.7 (Ref. 9) at 298 K) intermolecular potentials yield only reasonable agreement with experiment for the dielectric constant. Other popular rigid potentials, based on a transferable interaction potential (TIP), such as TIP2 (Ref. 10) ($\epsilon_r = 36$ at 300 K),⁶ and four-site potentials such as TIP4P (Ref. 11) ($\epsilon_r = 29$ (Ref. 6) at 300 K or alternatively 55 (Ref. 12) at 293 K) substantially under predict the dielectric constant. A recently modified four-site potential TIP4P/2005 ($\epsilon_r = 60$ at 298 K) (Ref. 13) yields agreement comparable to the SPC potential. Significant under or over prediction of the dielectric constant is also observed for *ab initio* potentials such as the Matsuoka–Clementi–Yoshimine MCY (Ref. 14) ($\epsilon_r = 57.3$ at 298 K) (Ref. 9) and NCC (Ref. 15) ($\epsilon_r = 100$ at 298 K) (Ref. 16) potentials. In contrast, a three-site potential TIP3P ($\epsilon_r = 96.9$ at 298 K),¹⁷ substantially over predicts the dielectric constant. The five-site TIP5P (Ref. 18) or TIP5P-E (Ref. 19) potential yield dielectric constants ($\epsilon_r \approx 80$ (Ref. 19) at 298.15 K), which are in good agreement with experiment. It should be noted that there is some variability in the dielectric constant reported in the literature for the various potentials, which partly reflects uncertainties arising from such factors as handling long-range interactions, cutoff values and appropriate equilibration periods. This is discussed in greater detail in Ref. 9.

A characteristic of many of these rigid body potentials is that they do not account for polarizability. The importance of polarizability in water is well known from earlier studies.²⁰ The addition of polarizability, such as in the SWM4-NNP ($\epsilon_r = 79$ at 298 K),²¹ MCYna ($\epsilon_r = 70.98$ at 298 K) (Ref. 9), and Gaussian charge polarizable model (GCPM) ($\epsilon_r = 84.3$ at 298 K) (Ref. 22) potentials results in improved predictions of the dielectric constant. Indeed, including polarizability in the force field of water is often considered necessary^{9,21–24}

^{a)} Author to whom correspondence should be addressed. Electronic mail: rsadus@swin.edu.au.

to improve the agreement with experiment for a wide range of properties and state points. Polarizable potentials approximate the effect of multibody interactions because the induced dipole of each molecule generates an electric field that affects all other molecules. However, polarizable potentials are generally much more computationally demanding than non-polarizable potentials,^{6,22} which greatly restricts their use for many applications.

The use of bond flexibility is increasingly discussed as an indirect and computationally less expensive way of introducing some polarizability effects,^{25–30} resulting in better agreement with experiment for some properties of water. Yu and Gunsteren³¹ identified three mechanisms for polarization arising from (a) electron redistribution, (b) changes in molecular geometry, and (c) molecule realignment in an electric field. Bond flexibility clearly impacts on the second of these three mechanisms. Early work of Dang and Pettitt²⁹ or Toukan and Rahman³⁰ showed that flexible versions of three-site water potentials accurately reproduced certain aspects of the vibrational motions of pure water. In a recent study, López-Lemus *et al.*²⁶ incorporated flexibility in the SPC/E potential and demonstrated that the calculated surface tensions and coexisting densities of water predicted by the flexible potential are closer to the experimental data than those of the rigid potential. The simple point charge flexible water SPC/Fw potential reported by Wu *et al.*²⁷ has resulted in a noticeable improvement in the accuracy of the viscosity, diffusion coefficient, and dielectric constant predicted at ambient conditions compared to the rigid SPC potential. In our earlier work,²⁸ we have shown that the flexible SPC/Fw potential also yields better predictions of saturation densities and the critical point than either the SPC or SPC/E potentials.

The use of flexible water potentials seems to be a promising alternative strategy for providing potentials that allow for the accurate simultaneous prediction of different properties. The aim of this work is to examine whether incorporating bond flexibility can be used to improve the prediction of the dielectric constant of water. In contrast to other work in the literature, which focuses mainly at ambient conditions, we are interested in examining the dielectric constant of water from ambient conditions up to supercritical temperatures and high pressures.

II. THEORY

A. Water potentials

In the SPC (Ref. 7) potential, the oxygen atom is represented as a partially charged Lennard-Jones bead, whereas the hydrogen atoms are simply represented by partial charges without any Lennard-Jones interactions. Water is modeled as a rigid molecule, with the relative positions of the three sites kept constant. The intermolecular interactions are calculated from

$$U_{\text{inter}} = \sum_i \sum_{j < i} \left\{ 4\epsilon_{ij} \left[\left(\frac{\sigma_{ij}}{r_{ij}} \right)^{12} - \left(\frac{\sigma_{ij}}{r_{ij}} \right)^6 \right] + \frac{q_i q_j}{r_{ij}} \right\}. \quad (1)$$

In their SPC/Fw potential, Wu *et al.*²⁶ added molecular flexibility to the SPC potential by accounting for intra-

molecular interactions,

$$U_{\text{intra}} = \sum \frac{K_{r,\text{OH}}}{2} (r_{\text{OH}} - r_{0,\text{OH}})^2 + \sum \frac{K_{\theta,\angle\text{HOH}}}{2} (\Theta_{\angle\text{HOH}} - \Theta_{0,\angle\text{HOH}})^2. \quad (2)$$

The Lennard Jones parameters ($\epsilon_{\text{OO}}/k_B = 78.197$, $\sigma_{\text{OO}} = 3.166 \text{ \AA}$, where k_B is the Boltzmann constant) and partial charges ($q_o = -0.82$, $q_H = 0.41$) in the SPC/Fw potential remain identical to those used in the SPC potential. The force constants ($K_r/k_B = 532881.6 \text{ K \AA}^{-2}$, $K_\theta/k_B = 38186.5 \text{ K rad}^{-1}$) and the equilibrium bond length ($r_{0,\text{OH}} = 1.012 \text{ \AA}$) and angle ($\theta_{0,\text{HOH}} = 113.24^\circ$) were only optimized to reproduce best the experimental dielectric constants at ambient conditions.

By comparing simulation results from the flexible SPC/Fw potential and the corresponding rigid SPC potential, we are able to investigate the effect of incorporating intramolecular degrees of freedom on the prediction of the densities, and dielectric constants of water. We also performed simulations for the rigid SPC/E potential⁵ that uses the same geometry and Lennard-Jones parameters as the SPC potential, with the addition of a self-polarization energy correction that slightly increases the partial charges ($q_o = -0.8476$, $q_H = 0.4238$). This means our simulations can yield insights into the effect of introducing polarization via both (a) intramolecular degrees of freedom and (b) increasing the partial charges.

B. Simulation details

The molecular dynamics simulations were performed³² in cubic boxes consisting of $N = 400$ molecules. The cutoff radius was set to 10 \AA , and standard long-range corrections to the Lennard-Jones energy and pressure were applied for all potentials using usual tail corrections.³ The Ewald sum was used to deal with the electrostatic interactions. The Ewald sum parameters were derived from an automatic parameter optimization,³² which yielded a convergence parameter of 0.3208 \AA^{-1} . The resulting k_{max} parameter was 8 in almost all cases, except for the 298 K/200 MPa ($k_{\text{max}} = 7$) and the 673 K/50 MPa ($k_{\text{max}} = 9$) state point. The values for all models were the same, which means that results for the different models are not influenced by different Ewald parameters. The trajectories were integrated by the velocity-Verlet algorithm. For each temperature and pressure, the systems were equilibrated for 2 ns in the Nosé–Hoover NpT ensemble to relax the system to thermodynamic equilibrium. After equilibration, 10 consecutive production runs, each of 500 ps, were performed to determine the average density, using the standard block average technique. Time steps of $\Delta t = 0.0005 \text{ ps}$ for the flexible SPC/Fw potential and $\Delta t = 0.001 \text{ ps}$ for the rigid potentials SPC and SPC/E were used. During the NpT -simulations, the coupling constants for the thermostat and the barostat were set to $\tau_T = 0.1$ and $\tau_\pi = 1.0$. These simulations yielded the density of water at a given temperature and pressure.

To determine the dielectric constants, we performed additional simulations in the Nosé–Hoover- NVT ensemble with a time step of $\Delta t = 0.001 \text{ ps}$ and a coupling constant of

$\tau_T = 0.5$ ps. The systems were again equilibrated for 2 ns at their averaged densities from the NpT -simulations, before performing production runs of 15 ns in the NVT ensemble, in which we saved the positions every 0.05 ps for further analysis. The dielectric constants was calculated from the fluctuation of the system's total dipole moment $M = \sum_i \mu_i$ by³³

$$\epsilon_\tau = 1 + \frac{4\pi}{3Vk_B T} (\langle M^2 \rangle - \langle M \rangle^2), \quad (3)$$

where the angled brackets denote ensemble averages.

III. RESULTS AND DISCUSSION

To extensively test the ability of the intermolecular potential to predict the dielectric constant, we performed simulations at both sub-critical temperatures (298.15 K and 473.15 K) and a super critical temperature (673.15 K) at pressures ranging from 0.1 MPa to 200 MPa. In performing these calculations, we were also able to determine the densities over these corresponding pressures and temperatures and the results are summarized in Table I.

A. Prediction of liquid and supercritical densities

The ability of an intermolecular potential to predict the pressure (p), temperature (T), and density (ρ) behavior of the fluid is an important requirement. At $T = 298.15$ K, $p = 0.1$ MPa, water has a density of 1 g cm^{-3} . The SPC/Fw ($\rho = 1.0099 \pm 0.0002 \text{ g cm}^{-3}$), SPC/E ($\rho = 0.9993 \pm 0.0003 \text{ g cm}^{-3}$) and SPC ($\rho = 0.9830 \pm 0.0041 \text{ g cm}^{-3}$) potentials come close to matching the experimental value with a deviation ranging between -1.4% and 1.3% . This good agreement with experiment can be at least partly attributed to the fact that the intermolecular potentials are specifically optimized for this ambient temperature state point.

A more severe test for an intermolecular potential is to examine its behavior over a range of temperatures and pressures. To the best of our knowledge, a wide-ranging $pT\rho$ study for these potentials has not been reported. The only partial exceptions are calculations for the vapor-liquid coexistence densities,^{2,28} which by definition, terminate at the critical pressure of approximately 22 MPa. Horn *et al.*³⁴ have reported densities for water between 235.5 K and 400 K for several TIP potentials (TIP3P, TIP4P, TIP4P-Ew, TIP4P-Pol2, and TIP5P). Comparison with experimental data indicated that there were significant deviations from the measured densities. The results obtained for the various TIP potentials also differed substantially.

The calculated densities at different temperatures and pressures ranging from 0.1 MPa to 200 MPa are compared with experimental data³⁵ in Figure 1 and Table I. At 298.15 K (Fig. 1(a)), the SPC/E potential yields very good agreement with experiment at all temperatures, whereas the SPC potential yields densities that are lower than the experimentally observed values. At both 473.15 K (Fig. 1(b)) and 673.15 K (Fig. 1(c)), the SPC/Fw densities are very close to the experimental values. Good, although slightly less accurate, agreement with experiment is also obtained for the SPC/E potential,

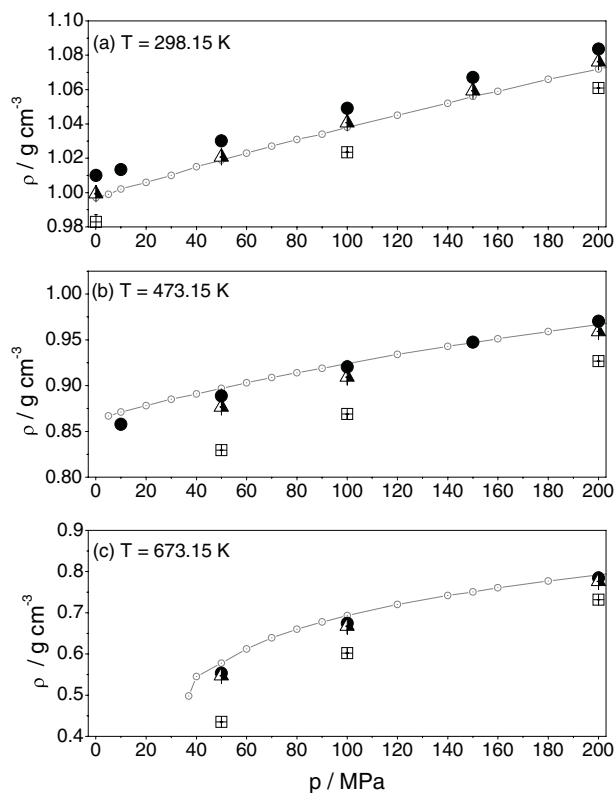


FIG. 1. Comparison of experimental densities (Ref. 35) (\circ) as a function of pressure with molecular dynamics calculations at temperatures of (a) 298.15 K, (b) 473.15 K, and (c) 673.15 K. Results are shown for the SPC/Fw (\bullet), SPC/E (\blacktriangle), and SPC (\boxplus) potentials. The line through the experimental points is only for guidance.

whereas the SPC potential predicts densities that are substantially lower. From these comparisons, we can infer that introducing bond flexibility in the SPC/Fw potential has a similar effect on the prediction of the densities as the increase of the partial charges in the rigid SPC/E potential, namely to yield higher densities that are in better agreement with the experimental data. However, at elevated temperatures we also observe that both the SPC/Fw and the SPC/E potential increasingly underestimate the experimental densities. This is consistent with our previously reported simulation results²⁸ for the prediction of the saturated liquid densities by these potentials.

B. The dielectric constant

As previously noted, there are often discrepancies in the literature for the dielectric constant attributed to an intermolecular potential. For example, at 292 K, the dielectric constant of the MCY potential was reported¹³ as $\epsilon_r = 34$, whereas a more recently obtained⁹ value at the slightly higher temperature of 298 K is $\epsilon_r = 57.30$. As discussed in Ref. 9, the source of such discrepancies has not been adequately resolved. However, it is now accepted that long simulation runs are required for the dielectric constants to converge, which may be a source of error in some earlier studies with limited computational resources. The importance of allowing for sufficient time for convergence is illustrated in Fig. 2, which compares the running ensemble averages of the dielectric

TABLE I. Experimental data (Ref. 35) and molecular simulation results for the densities and dielectric constants predicted by the SPC/Fw, SPC/E, and SPC potentials at different temperatures and pressures. The values in brackets represent the standard deviations.

T = 298.15 K								
Density (g cm^{-3})					Dielectric constant			
p/MPa	Expt.	SPC/Fw	SPC/E	SPC	Expt.	SPC/Fw	SPC/E	SPC
0.1	0.997	1.0099(0.0002)	0.9993(0.0003)	0.9830(0.0041)	78.36	78.1(1.6)	69.7(1.6)	63.2(0.9)
10	1.002	1.0140(0.0002)			78.72	78.2(1.6)		
50	1.019	1.0302(0.0003)	1.0207(0.0002)		80.20	78.8(1.6)	73.1(1.0)	
100	1.038	1.0491(0.0003)	1.0407(0.0001)	1.0235(0.0001)	81.92	82.1(1.9)	74.2(1.2)	70.6(1.0)
150	1.056	1.0671(0.0003)	1.0593(0.0002)		83.50	84.8(1.6)	75.9(1.3)	
200	1.072	1.0836(0.0002)	1.0762(0.0002)	1.0609(0.0001)	84.95	86(1.6)	77.7(1.9)	72.4(1.9)
T = 473.15 K								
Density (g cm^{-3})					Dielectric constant			
p/MPa	Expt.	SPC/Fw	SPC/E	SPC	Expt.	SPC/Fw	SPC/E	SPC
10	0.871	0.8577(0.0001)			35.23	35.1(0.2)		
50	0.897	0.8888(0.0009)	0.8768(0.0001)	0.8296(0.0002)	36.91	37.0(0.2)	35.1(0.2)	30.1(0.1)
100	0.924	0.9205(0.0006)	0.9094(0.0001)	0.8690(0.0001)	38.55	38.6(0.2)	36.9(0.3)	31.8(0.2)
150	0.947	0.9475(0.0004)			40.00	40.1(0.3)		
200	0.967	0.9703(0.0007)	0.9592(0.0010)	0.9268(0.0001)	41.28	41.8(0.3)	39.5(0.4)	34.3(0.2)
T = 673.15 K								
Density (g cm^{-3})					Dielectric constant			
p/MPa	Expt.	SPC/Fw	SPC/E	SPC	Expt.	SPC/Fw	SPC/E	SPC
50	0.524	0.5531(0.0017)	0.5473(0.0005)	0.4348(0.0007)	11.72	11.5(0.1)	11.7(0.1)	7.9(0.1)
100	0.693	0.6744(0.0010)	0.6676(0.0002)	0.6022(0.0003)	15.48	15.0(0.1)	14.9(0.1)	11.8(0.1)
200	0.792	0.7848(0.0009)	0.7760(0.0002)	0.7317(0.0002)	19.40	18.5(0.1)	18.4(0.1)	15.3(0.1)

constant of the SPC, SPC/E, and SPC/Fw potentials at 298.15 K and 0.1 MPa. The ensemble averages for ϵ_r of all potentials vary within the range of their uncertainties only for simulation runs longer than 13 ns.

Prior to examining the different potentials over a wide range of temperatures and pressures, we checked the reliability of our simulations by comparing our results with corresponding data from literature at 298.15 K and 0.1 MPa. Our value ($\epsilon_r = 78.1 \pm 1.6$) for the SPC/Fw potential is also consistent with a previously reported²⁷ value ($\epsilon_r = 79.63 \pm 1.62$)

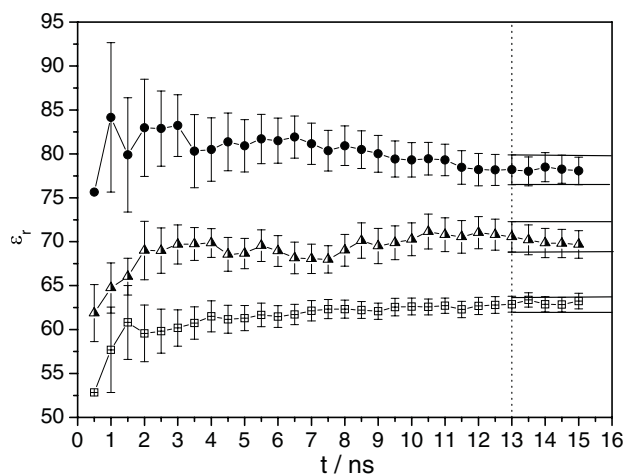


FIG. 2. Ensemble average of the dielectric constant of water at 298.15 K and 0.1 MPa, determined every 0.5 ns in a simulation run of at least 15 ns. Results from molecular dynamics simulations for the SPC/Fw (●), SPC/E (▲), and SPC (■) potentials.

within the range of uncertainties. For both, the SPC and the SPC/E potential, the reported simulations for the dielectric constants^{8,9,36–39} at ambient conditions in the literature vary significantly. This can be attributed to different treatments of the long range cutoff as well as to different, and possibly inadequate, simulation lengths.⁹ Our result ($\epsilon_r = 69.7 \pm 1.6$) for the dielectric constant of the SPC/E potential at 298.15 K and 0.1 MPa lies in the range of reported data varying from 63.7 (Ref. 6) to 76.7.²³ It is also in good agreement with values given by Svishchev *et al.*³⁸ and Höchtl *et al.*³⁷ The reported simulation results for the ϵ_r of the SPC potential vary between 54 and 72 (Ref. 40) and again, our result ($\epsilon_r = 63.2 \pm 0.9$) lies within this range. The good agreement between our results at ambient conditions and values from literature for all potentials gives us confidence that our simulations can also provide reliable predictions at elevated pressures and temperatures that have rarely been studied by molecular simulation.

Results obtained for the dielectric constant at elevated temperatures and pressures are summarized in Table I and comparisons with experimental data³⁵ are given in Figure 3. At 298.15 K (Fig. 3(a)) and 473.15 K (Fig. 3(b)), the dielectric constant predicted by the SPC/Fw potential almost coincides with the experimental data at some pressures. In contrast, the dielectric constant is noticeably under predicted by both the SPC/E and SPC potentials, with the SPC potential yielding a typical discrepancy of greater than 15%. The results for the SPC/Fw potential at 673.15 K (Fig. 3(c)) start to display small under predictions but the accuracy is nonetheless acceptable. In this case, the quality of the predictions for the SPC/E potential is of similar accuracy whereas the inaccuracy of the SPC potential is typically greater than 20%.

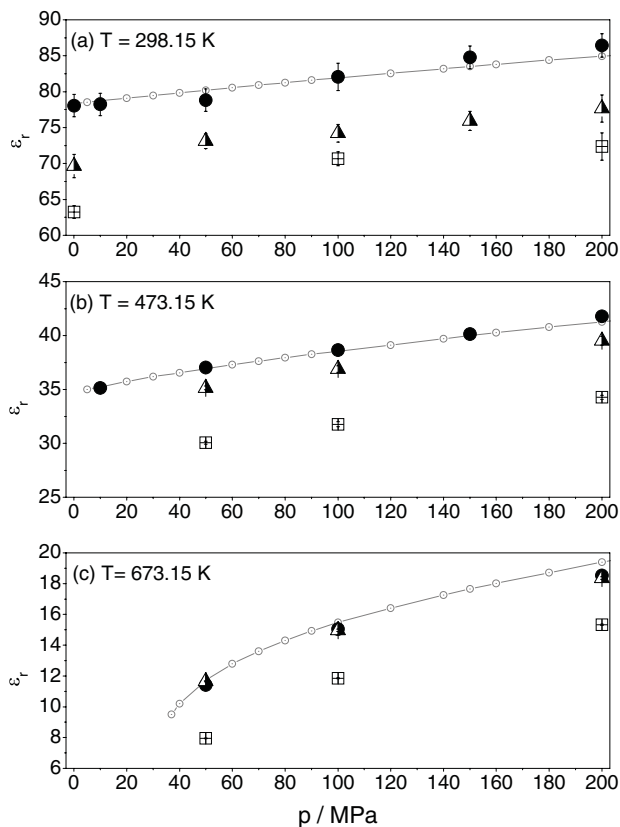


FIG. 3. Comparison of experimental dielectric constants (Ref. 35) (\circ) as a function of pressure with molecular dynamics calculations at temperatures of (a) 298.15 K, (b) 473.15 K, and (c) 673.15 K. Results are shown for the SPC/Fw (\bullet), SPC/E (\blacktriangle), and SPC (\boxplus) potentials. The line through the experimental points is only for guidance.

It is apparent from the above comparison that introducing bond flexibility in the SPC/Fw potential considerably improves the prediction of the dielectric constant by correcting for the under prediction in the rigid SPC potential. The increase of the partial charges in the rigid SPC/E also yields higher values for the dielectric constants, which is most effective at supercritical temperatures (Fig. 3(c)). These observations are in agreement with the findings of Wasserman *et al.*³⁶ that the SPC/E potential can only be used to predict the dielectric constant of water at densities up to 1 g cm^{-3} , whereas it tends to yield ϵ_r values that are too low at higher densities. The SPC/Fw potential however gives a very good reproduction of the experimental dielectric constants over the entire range of temperatures and pressures studied here, with an averaged deviation from the experimental values of 0.9% in the liquid and 3.1% in the supercritical phase. This suggests that the SPC/Fw potential could be very useful for studies of electrolyte solutions.

C. Impact of flexibility

Introducing bond flexibility in the SPC/Fw potential means that the dipole moment can vary in response to the thermodynamic state point. Figure 4 shows the absolute values of the molecular dipole moments of the SPC/Fw potential as a function of both temperature and pressure. For comparison, the dipole moments for the SPC and SPC/E fluids

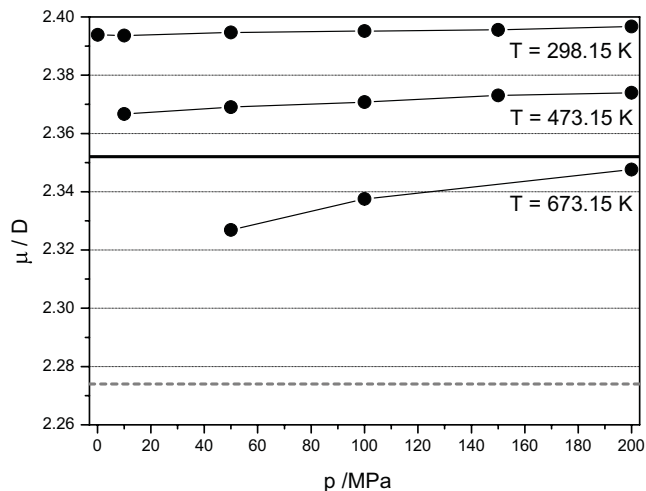


FIG. 4. The molecular dipole moments of the flexible SPC/Fw potential as a function of temperature and pressure. For comparison, the constant molecular dipole moments of the rigid SPC and SPC/E potentials are $\mu_{\text{SPC}} = 2.274 \text{ D}$ and $\mu_{\text{SPC/E}} = 2.352 \text{ D}$ and are shown as dashed gray and black lines, respectively. The lines through the data points are for guidance only.

are $\mu_{\text{SPC}} = 2.274 \text{ D}$ and $\mu_{\text{SPC/E}} = 2.352 \text{ D}$, respectively, at all temperatures and pressures. It is apparent from this comparison that bond flexibility increases the molecular dipole moment, which may in turn result in a higher system dipole moment and higher values for the dielectric constants. Figure 4 also indicates that bond flexibility allows the molecular dipole moment to change with the thermodynamic state point, and thereby mimic the change of the intermolecular interactions in response to the local environment. This observation supports other studies^{26,41} that have concluded that introducing flexibility transforms a rigid water potential into a polarizable potential, in agreement with the geometric polarization mechanism identified by Yu and van Gunsteren³¹ as discussed above.

We determined the equilibrium geometry of the SPC/Fw fluid at different state points. Namely, the high density liquid phase at 298.15 K at both 0.1 MPa (state I: $r_{\text{OH}} = 1.0310 \text{ \AA}$, $\Theta_{\text{HOH}} = 107.70^\circ$, $Q_T = 2.046 \text{ D \AA}$) and 50 MPa (state II: $r_{\text{OH}} = 1.0312 \text{ \AA}$, $\Theta_{\text{HOH}} = 107.68^\circ$, $Q_T = 2.046 \text{ D \AA}$); the liquid phase at the elevated temperature of 473.15 K and 50 MPa (state III: $r_{\text{OH}} = 1.0271 \text{ \AA}$, $\Theta_{\text{HOH}} = 108.21^\circ$, $Q_T = 2.043 \text{ D \AA}$); and the supercritical phase at 673.15 K and 50 MPa (state IV: $r_{\text{OH}} = 1.0228 \text{ \AA}$, $\Theta_{\text{HOH}} = 109.30^\circ$, $Q_T = 2.062 \text{ D \AA}$). The “quadrupole moment” (Q_T) at these states was calculated from the following relationship⁴²

$$Q_T = \frac{3(r_{\text{OH}} \sin \theta)^2}{4r_{\text{OH}} \cos \theta} \mu, \quad (4)$$

where 2θ is the H–O–H angle.

The results show that the equilibrium bond lengths (r_{OH}) of the SPC/Fw fluid at the various states are significantly larger than both the model’s parameter ($r_{0,\text{OH}}$) and also that of the bond length of the rigid SPC potential with $r_{\text{OH}} = 1 \text{ \AA}$. However, the equilibrium the H–O–H bond angles are remarkably smaller than the bond angle potential parameter for both the SPC/Fw ($\Theta_{0,\text{HOH}} = 113.24^\circ$) and the rigid SPC and SPC/E potentials ($\Theta_{0,\text{HOH}} = 109.47^\circ$). Both the elongation of

the equilibrium O–H bonds and the smaller equilibrium bond angles contribute to the larger molecular dipole moments of the flexible SPC/Fw potential compared to the rigid SPC potential with the same point charges. The change in the geometry at the different state points also leads to a change in the strength of the quadrupolar interactions. The molecular quadrupole moments of the SPC/Fw potential are larger than the values obtained for either the SPC potential ($Q_{T,SPC} = 1.969 \text{ D \AA}$) or the SPC/E potential ($Q_{T,SPC/E} = 2.0368 \text{ D \AA}$). In the optimization of their SPC/Fw potential, Wu *et al.*²⁷ studied the influence of the bond angle and bond length on the dielectric constant at ambient conditions, and observed that this property is strongly sensitive to bond angle changes. This influence appears to be reflected in our calculations.

The equilibrium bond lengths of the SPC/Fw potential contract with increasing temperature (i.e., decreasing densities, states II–IV), whereas the equilibrium bond angles expand, both leading to a decrease of the molecular dipole moment. However, whereas the decrease of the equilibrium bond length lowers the quadrupole moment, the expanding H–O–H angle increases it. In the liquid phase (states I, II, and III) both effects nearly balance each other, so that there is little change to the quadrupole moments of the SPC/Fw potential. The decrease of the molecular dipole moment with increasing temperature results in lower dielectric constants from the SPC/Fw potential whereas the slightly smaller quadrupole moments counteract it. In the supercritical phase at 673.15 K (state IV), the increase of the quadrupolar interaction with the expanded bond angle is more pronounced than its decrease with the smaller equilibrium O–H bond. In state IV both effects, the smaller dipole moments and the higher quadrupole moments, lower the dielectric constants of the SPC/Fw potential as a result of reduced dipole–dipole correlations.²⁷

IV. CONCLUSIONS

The flexible SPC/Fw potential by Wu *et al.*²⁷ yields very good agreement with experiment for dielectric constants over the entire range of state points, and it is superior to all other potentials studied in this work. We found that the SPC/Fw potential show elongated equilibrium O–H bonds compared to the rigid potential, whereas the equilibrium bond angle decreases below the value of the SPC or SPC/E potential. Both effects result in higher molecular dipole moments of the flexible SPC/Fw potential compared to the SPC potential with the same point charges. When the temperature is increased (i.e. at decreasing densities), the O–H bonds of the flexible potentials slightly contract but remain elongated compared to the rigid potentials. In contrast, the equilibrium H–O–H bond angles increase with temperature. The changes in geometry in response to the thermodynamic state point allow both the molecular dipole moment and the quadrupole moment to vary.

The introduction of bond flexibility improves the calculation of both the dielectric constant and density over a wide range of state points. The increase in the density is probably mainly attributed to bond length elongation, whereas the dielectric constant is sensitive to changes in the equilibrium

bond angle, due to its impact on both the molecular dipole and quadrupole moment.

- ¹D. Eisenberg and W. Kauzmann, *The Structure and Properties of Water* (Clarendon, Oxford, 2005); E. Brunner, M. C. Thies, and G. M. Schneider, *J. Supercrit. Fluid* **39**, 160 (2006); V. M. Shmonov, R. J. Sadus, and E. U. Franck, *J. Phys. Chem.* **97**, 9054 (1993); A. E. Mather, R. J. Sadus, and E. U. Franck, *J. Chem. Thermodyn.* **25**, 771 (1993).
- ²R. J. Sadus, *Molecular Simulation of Fluids: Theory, Algorithm and Object-Orientation: Theory, Algorithms and Object-Orientation* (Elsevier, Amsterdam, 1999).
- ³A. A. Chialvo and P. T. Cummings, *Adv. Chem. Phys.* **109**, 115 (1999).
- ⁴*CRC Handbook of Chemistry*, 80th ed., Edited by R. C. West (CRC, Boca Raton, 2005).
- ⁵H. J. C. Berendsen, J. R. Grigera, and T. P. Straatsma, *J. Phys. Chem.* **91**, 6269 (1987).
- ⁶H. J. Strauch and P. T. Cummings, *Mol. Simul.* **2**, 89 (1989).
- ⁷H. J. C. Berendsen, J. P. M. Postma, W. F. van Gunsteren, and J. Hermans, in *Intermolecular Forces*, edited by B. Pullman (Reidel, Dordrecht, 1981).
- ⁸M. R. Reddy and M. Berkowitz, *Chem. Phys. Lett.* **155**, 173 (1989).
- ⁹J. Li, Z. Zhou, and R. J. Sadus, *J. Chem. Phys.* **127**, 154509 (2007).
- ¹⁰W. L. Jorgensen, *J. Chem. Phys.* **77**, 4156 (1982).
- ¹¹W. L. Jorgensen and J. D. Madura, *Mol. Phys.* **56**, 1381 (1985).
- ¹²M. Neumann, *J. Chem. Phys.* **85**, 1567 (1986).
- ¹³J. L. F. Abascal and C. Vega, *J. Chem. Phys.* **123**, 234505 (2005).
- ¹⁴O. Matsuoka, E. Clementi, and M. Yoshimine, *J. Chem. Phys.* **64**, 1351 (1976).
- ¹⁵U. Niesar, G. Corongiu, E. Clementi, G. R. Kneller, and D. K. Bhat-tacharya, *J. Chem. Phys.* **94**, 7949 (1990).
- ¹⁶J.-C. Soetens, M. T. C. Martins Costa, and C. Millot, *Mol. Phys.* **94**, 577 (1998).
- ¹⁷W. L. Jorgensen, J. Chandrasekhar, J. D. Madura, R. W. Impey, and M. L. Klein, *J. Chem. Phys.* **79**, 926 (1983).
- ¹⁸M. W. Mahoney and W. L. Jorgensen, *J. Chem. Phys.* **112**, 8910 (2000).
- ¹⁹S. W. Rick, *J. Chem. Phys.* **120**, 6085 (2004).
- ²⁰M. Sprik and M. L. Klein, *J. Chem. Phys.* **89**, 7556 (1988).
- ²¹G. Lamoureux, E. Harder, I. V. Vorobyov, B. Roux, and A. D. MacKerell, Jr., *Chem. Phys. Lett.* **418**, 245 (2006).
- ²²P. Paricaud, M. Predota, A. A. Chialvo, and P. T. Cummings, *J. Chem. Phys.* **122**, 244511 (2005).
- ²³I. M. Svishchev, P. G. Kusalik, J. Wang, and R. J. Boyd, *J. Chem. Phys.* **105**, 4742 (1996).
- ²⁴I. M. Svishchev and T. M. Hayward, *J. Chem. Phys.* **111**, 9034 (1999).
- ²⁵T. I. Mizan, P. E. Savage, and R. M. Ziff, *J. Comput. Chem.* **17**, 1757 (1996).
- ²⁶J. L6pes-Lemus, G. A. Chapela, and J. Alejandre, *J. Chem. Phys.* **128**, 174703 (2008).
- ²⁷Y. Wu, H. L. Tepper, and G. A. Voth, *J. Chem. Phys.* **124**, 024503 (2006).
- ²⁸G. Raabe and R. J. Sadus, *J. Chem. Phys.* **126**, 044702 (2007).
- ²⁹L. X. Dang and B. M. Pettitt, *J. Phys. Chem.* **91**, 3349 (1987).
- ³⁰K. Toukan and A. Rahman, *Phys. Rev. B* **31**, 2643 (1985).
- ³¹H. Yu and W. F. van Gunsteren, *Comput. Phys. Commun.* **17**, 69 (2005).
- ³²W. Smith and T. R. Forester, *The DL_POLY Molecular Simulation Package* (2009) http://www.cse.clr.ac.uk/mis/software/DL_POLY.
- ³³M. Neumann, *Mol. Phys.* **50**, 841 (1983).
- ³⁴H. W. Horn, W. C. Swope, J. W. Pitera, J. D. Madura, T. J. Dick, G. L. Hura, and T. Head-Gordon, *J. Chem. Phys.* **120**, 9665 (2004).
- ³⁵R. Deul, *Dielektrizit6tskonstante und Dichte von Wasser-Benzol-Mischungen bis 400°C und 3000 bar*, Ph.D. dissertation, University of Karlsruhe, Karlsruhe, Germany (1984).
- ³⁶E. Wasserman, B. Wood, and J. Brodholdt, *Geochim. Cosmochim. Acta* **56**, 1 (1995).
- ³⁷P. H6chtl, S. Boresch, W. Bitomsky, and O. Steinhauser, *J. Chem. Phys.* **109**, 4927 (1998).
- ³⁸I. M. Svishchev and P. G. Kusalik, *J. Chem. Phys.* **98**, 728 (1994).
- ³⁹A. Gl6tti, C. Oostenbrink, X. Daura, D. P. Geerke, H. Yu, and W. F. van Gunsteren, *Braz. J. Phys.* **34**, 116 (2004).
- ⁴⁰W. L. Jorgensen and C. Jenson, *J. Comput. Chem.* **19**, 1179 (1998).
- ⁴¹C. C. Liew, H. Inimata, and K. Arai, *Fluid Phase Equilib.* **144**, 287 (1998).
- ⁴²S. Chatterjee, P. G. Debenedetti, F. H. Stillinger, and R. M. Lynden-Bell, *J. Chem. Phys.* **128**, 124511 (2008).